Endocrine, *vol. 7, no. 3, 367–375, December 1997* 0969-711X/97/7:367-375/$10.25

Quantitative Measurement of Islet Glucagon Response to Hypoglycemia by Confocal Fluorescence Imaging in Diabetic Rats:

Effects of Phlorizin Treatment

Krishna S. Rastogi, Robin L. Cooper, Zhi Q. Shi, and Mladen Vranic

Departments of [1]Physiology and [2]Medicine, Faculty of Medicine, University of Toronto, Toronto, Ontario, Canada

We have shown that the glucagon irresponsiveness to hypoglycemia in diabetic rats is markedly improved by correction of hyperglycemia independent of insulin. In contrast, normalization of glycemia by insulin did not improve this response. To find out whether these glucagon responses reflect changes in islet glucagon, we directly quantified glucagon area and content in each pancreatic islet by using fluorescent immunostaining and computerized image analysis with confocal laser scanning microscopy (CLSM). The pancreases were analyzed in four groups of rats.

1. **Normal controls (NC, $n = 4$), streptozotocin (65 mg/kg) diabetic rats.**
2. **Diabetic untreated (DU, $n = 4$).**
3. **Diabetic Phlorizin-treated, (0.4 g/kg), twice daily for 4 d (DP, $n = 4$).**
4. **Diabetic insulin-treated, using sustained release (2–3 U/d) insulin implant for 5 d (DI, $n = 4$).**

Basal plasma glucose was 7.4 ± 0.3 m*M* in NC, increased to 14.5 ± 2.2 m*M* in DU, which was normalized in DP (5.5 ± 0.5) and DI (6.7 ± 0.8). Acute hypoglycemia (H) was induced by iv insulin injection. The rats were sacrificed 2 h after insulin injection and the pancreas was removed. By imaging with CLSM, we quantified:

1. **Percent of glucagon containing A-cell area/islet area,**
2. **Fluorescence intensity per islet area, which indicated glucagon content in the islet.**
3. **Fluorescence intensity per glucagon area indicating glucagon concentration in A-cells.**

In NC, glucagon containing A cell area was 21 ± 2% of the islet area, and glucagon intensity and concentration was 11 ± 1 U and 36 ± 3.0 U, respectively, in basal (O) state and did not change in (H). In DU, glucagon area increased 183% (O) and 166% (H), and islet glucagon intensity increased by 235% (O) ($p < 0.05$), but decreased to 135% in H. Glucagon area in DP and DI did not differ significantly from DU. However, hypoglycemia in DP increased glucagon intensity in islet further to 306% of normal control ($p < 0.05$), suggesting marked increase in glucagon content indicating increased synthesis. In contrast, DI compared to DP showed a decrease in glucagon intensity in islet (46 ± 3, DP to 22 ± 2 DI; $p < 0.05$) in (H) state. Glucagon concentration followed the same pattern as its intensity. Conclusion:

1. **Increase in islet glucagon content in diabetic rats was associated with increase in glucagon containing A-cell area per islet.**
2. **Phlorizin-induced insulin independent correction of hyperglycemia increased glucagon content per islet in hypoglycemic state. This, in part, probably contributed to improved glucagon response to hy poglycemia observed earlier**
3. **Normalization of glycemia with insulin reduced glucagon content of each islet during hypoglycemia.**

This may explain, in part, unresponsiveness of glucagon to hypoglycemia often observed in insulin-dependent diabetes mellitus (IDDM) with intensive insulin therapy.

Key Words: Islet glucagon; hypoglycemia; confocal fluorescence; diabetic rats; phlorizin.

Received July 17, 1997; Revised October 3, 1997, Accepted October 9, 1997.

Author to whom all correspondence and reprint requests should be addressed: Dr. M. Vranic, Department of Physiology, Medical Sciences building, Room 3358, University of Toronto, Toronto, Canada, M5S 1A8. E-mail: mladen.vranic@utoronto.ca

Introduction

It is well known that in both insulin-dependent diabetes mellitus (IDDM) and alloxandiabetic dogs *(1–6)*, there is

impaired glucose counterregulation during insulin-induced hypoglycemia. This impairment is primarily ascribed to defective glucagon release and, therefore, defective glucose production. Such a defect limits intensive insulin therapy in IDDM patients. Similar defects have been documented in streptozotocin diabetic rats *(7,8)*.

The mechanism responsible for the defective glucagon responsiveness has not yet been fully clarified. We have previously shown that acute normalization of glycemia using insulin in dogs resulted in a paradoxical decrease in pancreatic glucagon/somatostatin ratio *(9)*. We suggested that this marked fall in glucagon content relative to somatostatin in insulin-induced normoglycemia might explain, in part, the impaired glucagon responsiveness to hypoglycemia in diabetic dogs *(9,10)*. The defect may also be in the glucose sensing mechanism of the A-cells of the pancreatic islet. Persistent hyperglycemia may desensitize A-cells and B-cells to glycemic fluctuations *(11–14)*. Normalization of glycemia by phlorizin treatment, independent of insulin, partially restored the decremental glucagon response to acute hyperglycemia *(15)*, improved hepatic glucose production to insulin-induced hypoglycemia in diabetic dogs *(5,6)*, and normalized tissue insulin sensitivity in diabetic rats *(16)*. In streptozotocin diabetic rats, we demonstrated that chronic normalization of hyperglycemia using phlorizin independently of insulin significantly improved glucagon responsiveness to acute hypoglycemia, whereas normalization of glycemia with insulin treatment failed *(7)*, analogous to the observations in IDDM patients kept on tight glycemic control with insulin *(4,17)*. It has been suggested that exogenous insulin exerts an inhibitory effect on glucagon secretion *(18,19)*.

Glucagon responsiveness has been traditionally assessed by changes in circulating glucagon levels. The changes in islet glucagon content, which reflects more closely the dynamic hormone response to the metabolic milieu, are pursued in the present study for the first time by a new methodology that assesses glucagon content directly in pancreatic A-cells. By using fluorescent-labeled antibodies that specifically recognized glucagon and imaging with a confocal laser scanning microscope (CLSM), we have been able to measure quantitatively:

1. Cross-sectional area of islets and of individual glucagon-staining A-cell area.
2. Fluorescence intensity of entire islet indicating glucagon content per islet.
3. Fluorescence intensity of glucagon containing A-cell area in islet indicating glucagon concentration in A-cells.

We utilized relative intensity measurements to demonstrate differences in glucagon level. Thus, this unique combination of the use of immunocytochemistry and confocal microscopy allowed us to measure relative differences in glucagon levels of pancreatic islets. Previously *(7)* we measured glucagon content in the pancreas, which, however, does not yield information on the islet glucagon content or concentration. In streptozotocin diabetic rats, it was previously shown *(20,21)* that total glucagon content of pancreas increased marginally or not at all, but glucagon content of diabetic islet increased markedly. This was found to be mainly owing to 50–70% loss of islets in diabetic rat pancreas *(21,22)*. Marked reduction in islet number has also been reported in type I diabetes in human *(21)* as well as in dogs by us *(8,9)*. In addition, a very small percentage of islets (1–3%) occupy the total pancreatic mass. In previous studies, we used acid alcohol extraction to separate peptide hormones in pancreas and then measured glucagon by radioimmunology (RIA) in neutral extracts *(7)*. A small number of islets dispersed in a relatively large pancreatic mass would dilute tissue hormone content, and differences between treatment groups would be difficult to quantify. With new methodology, we wanted to quantify the glucagon content at the level of the islet. On completion of our previous study *(7)*, the confocal fluorescence imaging technology became available to us. Thus, we decided to pursue further our investigation of the glucagon responsiveness to hypoglycemia at the islet level. This new methodology has been applied to the pancreas of four groups of rats reported previously. The groups are normal control rats, untreated diabetic rats, phlorizin-treated diabetic rats, and insulin-treated diabetic rats in basal state as well as after insulin-induced hypoglycemia. These data further extend the understanding of the cellular mechanism of impaired glucagon response to hypoglycemia in diabetic rats and the impact of glycemic changes on the islet glucagon content, which reflects the net balance between the hormone synthesis and release.

Results

Localization of A-Cells by CLSM Analysis

By using fluorescent-labelled antibodies that recognize glucagon and by imaging with a CLSM, we have been able to form a composite of 8–10 scans at 1-μm optical sections from 10-μm thick tissue at various focal planes into a single image for quantitative measures. Even after accumulation and averaging of 8–10 scans, no attenuation of fluorescence signal was noted. Use of the antifading agent phenylenediamine largely prevented fading of the fluorescence caused by laser light excitation. All islets in a pancreatic section were scanned. It was found that strongly fluorescent (red, yellow, and green) islet was surrounded by weakly (negligible) fluorescent (dark blue) acinar cells, since red denoted the maximum intensity, followed by yellow, green, light blue, and dark blue. Figure 1 shows representative sections from each group. The composite digitized image of the islet of normal rat revealed that glucagon staining was most intense within the boundaries of the islet (Fig. 1A), thus indicating that glucagon-containing A-cells are localized in the peripheral region of the islet, where A- cells are known to reside. The pattern of distribu-

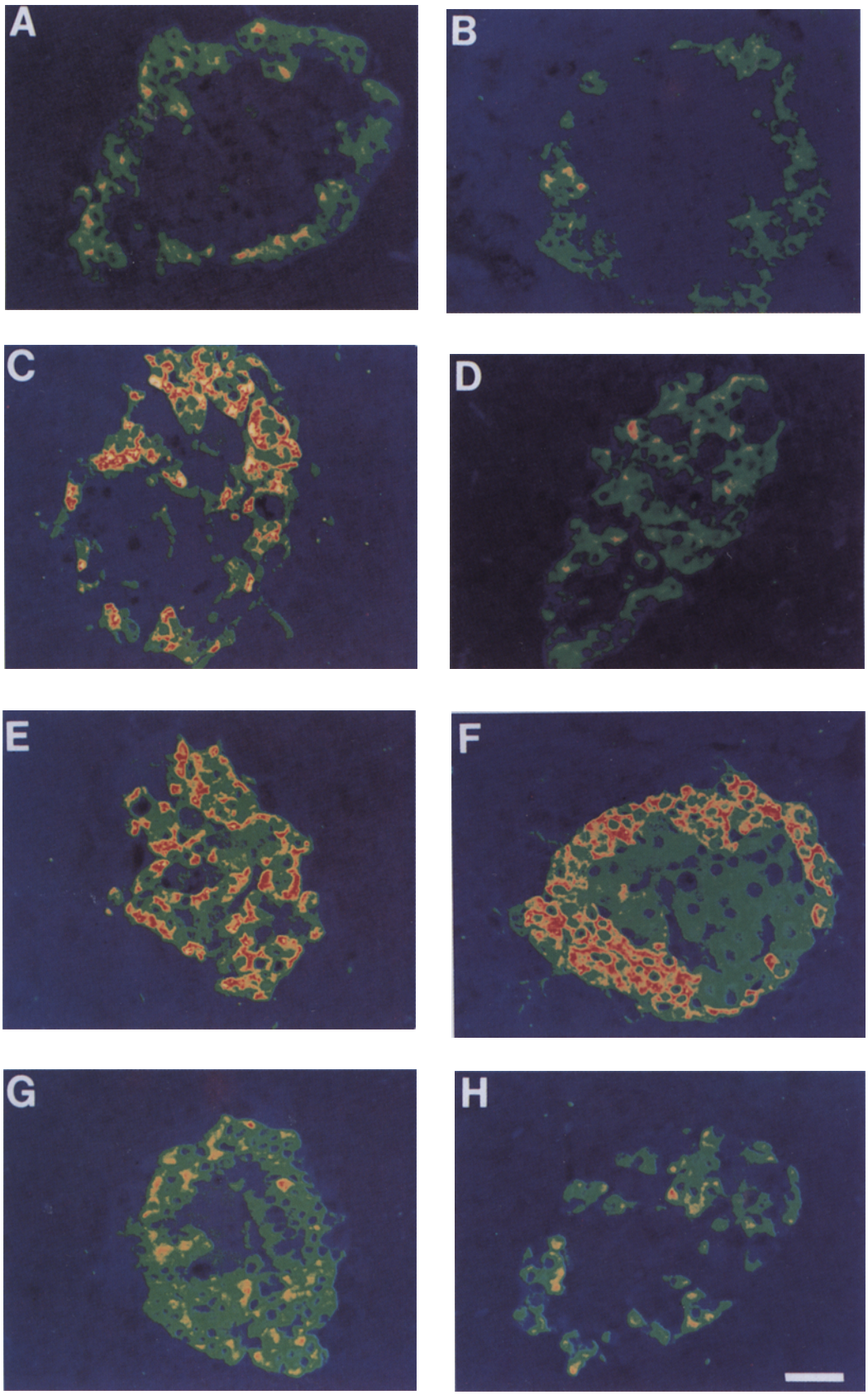

Fig. 1. Confocal images of normal and diabetic rat islets. **(A)** Normal islet in basal state. **(B)** Normal islet in hypoglycemic state. **(C)** Diabetic islet in basal state. **(D)** Diabetic islet in hypoglycemic state. **(E)** Diabetic phlorizin-treated islet in basal state. **(F)** Diabetic phlorizin-treated islet in hypoglycemic state. Note increase in red area (maximum) indicating chronic hyperplasia and increase in glucagon content. **(G)** Diabetic insulin-treated islet in basal state. **(H)** Diabetic insulin-treated islet in hypoglycemic state. Insulin treatment compared to phlorizin treatment showed a decrease in fluorescence intensity (green and yellow) indicating reduced glucagon content. Images are rendered in pseudocolor for visual assessment. Red denotes the maximum intensity, followed by yellow, green, light blue, and dark blue.

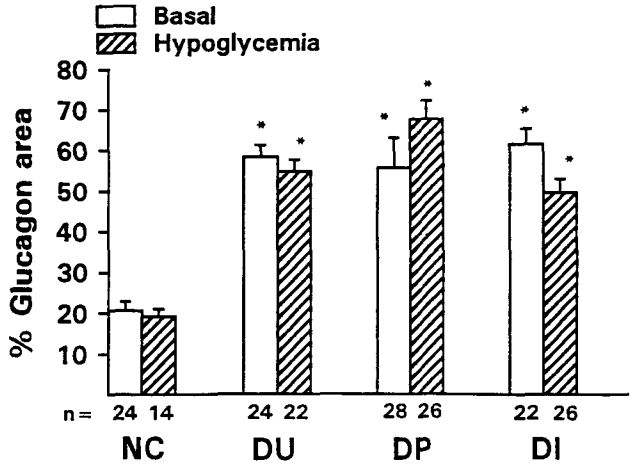

Fig. 2. Morphometric quantitation of glucagon area as a percent of total islet area in pancreas of normal control (NC), diabetic untreated (DU), diabetic phlorizin-treated (DP), and diabetic insulin-treated (DI) rats in basal state (open bars) and after acute insulin-induced hypoglycemia (hatched bars). Each group consisted of 4 rats and *n* is the total number of islets measured in each group. $*p < 0.05$. Free star indicates comparison with basal NC group.

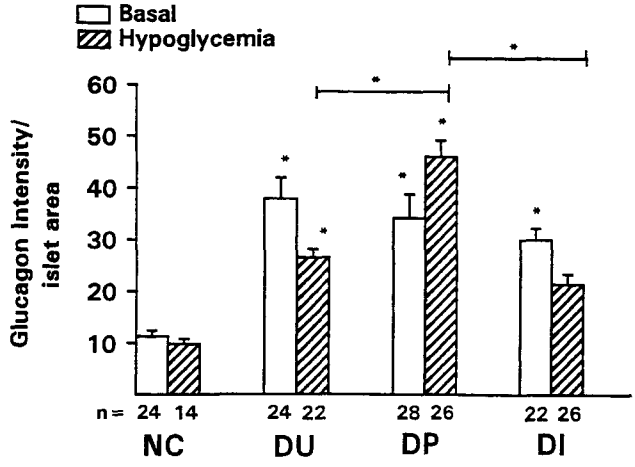

Fig. 3. Comparison of glucagon fluorescent intensity per islet area in basal (open bars) and hypoglycemic state (hatched bars) in normal control (NC), diabetic untreated (DU), diabetic phlorizin-treated (DP), and diabetic insulin-treated rats (DI). Fluorescence intensities of glucagon in islets were quantified by CLSM. Graph shows mean islet fluorescence intensity expressed as gray scale units. Each group consisted of 4 rats, and *n* is the total number of islets measured in each group. $* p < 0.05$. Comparison between the two groups is indicated by a horizontal line, and free star indicates comparison with basal NC group.

tion of A-cell remained unchanged after hypoglycemia in normals (Fig. 1B).

Examination of the islets of diabetic rat showed disruption of normal islet architecture. There was marked increase in glucagon-containing A-cells (Fig. 1C), which were scattered throughout the islet, in contrast to the peripheral location in the normal islet. In the diabetic hypoglycemic islet, the distribution of the A-cell remained the same, although the intensity of fluorescence was low (Fig. 1D). Normalization of glycemia with phlorizin showed higher glucagon staining fluorescence than normal rats in basal state (Fig. 1E) and marked further increase in red area (maximum) after hypoglycemia (Fig. 1F). However, when blood glucose of diabetic rats was normalized with insulin, compared to DP, there appeared to be much less intensity of glucagon fluorescence in A-cells (green and yellow) (Fig. 1G), and also distribution of the glucagon-containing A-cell was less in islets after insulin-induced hypoglycemia (Fig. 1H).

Quantification of Glucagon Area and Intensity

Morphometric quantitation showed that in normal control rats, mean glucagon area was 20.5 ± 2.2% of the total islet area in the basal state which did not differ from 19.2 ± 1.8% in the hypoglycemic state (Fig. 2). In the untreated diabetic rats, there was a 2.8-fold (184%) increase in the basal state (58.3 ± 2.9%) and 2.7-fold (167%) in the hypoglycemic condition (54.7 ± 2.9%) (both $p < 0.05$ compared to the normal controls). Similar increments in A-cell area were also observed in phlorizin (55.6 ± 3.4, DPO and 67.6 ± 4.5% DPH) and insulin-treated (61.5 ± 3.8 D10 and 49.6 ± 3.4 DIH) rats. These increments were significantly different from normal controls, but as expected, not from untreated diabetic rats ($p < 0.05$).

Quantification of the immunofluorescence intensity of glucagon in the confocal images are shown in Fig. 3 and expressed as total glucagon intensity per islet area (average intensity). Measurement of the same area of acinar tissue as islet area showed constant background intensity in all the groups studied. There was no significant difference in glucagon intensity (content) in the normal group before and after insulin-induced hypoglycemia (Fig. 3). Glucagon intensity markedly increased in all diabetic groups, compared to the normal group as also seen visually in Figs. 1A–G. Glucagon intensity was more than threefold higher in the untreated diabetic group compared to the normal group (37.9 ± 4.1, DUO, vs 1 1.3 ± 1 .2, NCO, $p < 0.05$). Normalization of glycemia with phlorizin resulted in a marked increase in glucagon intensity during hypoglycemia (45.9 ± 3.2, DPH), which was fourfold greater than that of normal controls. In contrast, in uncontrolled diabetes and in insulin-treated diabetes, glucagon intensity was low (26.6 ± 1.6, DUH and 21.5 ± 1.9, DHM). Thus, compared to DP during hypoglycemia, glucagon intensity was significantly higher than in DU and DI ($p < 0.05$). This is also seen visually in Fig. 1 (B,D,H). These data report for the first time that hypoglycemia increased glucagon content only in phlorizin, but not in insulin-treated or untreated rats. Since glucagon area did not change with various treatments, glucagon intensity per glucagon area (Fig. 4), indicating concentration of glucagon per A cell, followed the same pattern as glucagon intensity per islet area (Fig. 3). During hypoglycemia, glucagon intensity per glucagon area was significantly higher ($p < 0.05$) in DP (62.7 ± 2.8, DPH) than in controls

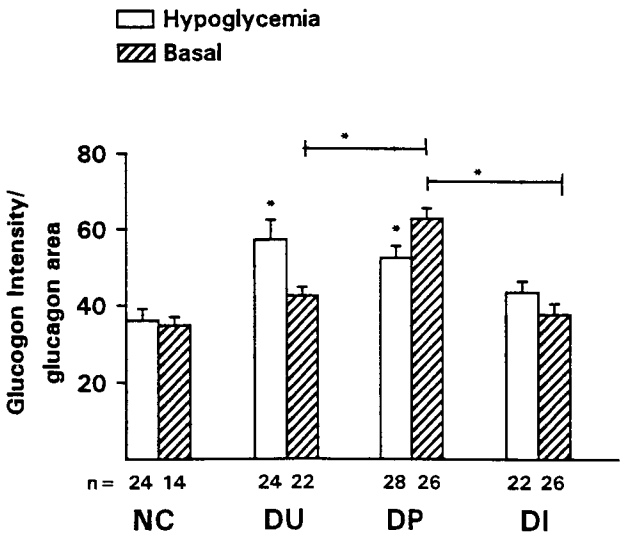

Fig. 4. Comparison of glucagon concentration in A-cells of islets as indicated by glucagon fluorescence intensity per glucagon containing A-cell area in the islet. Experimental groups and number of rats are the same as in Fig. 4. *n* is the total number of islets measured in each group. * $p < 0.05$. Comparison between the two groups is indicated by a horizontal line, and free star indicates comparison with basal NC group. DUO vs DIH, DPO vs DIH, and DPH vs DIO were also significant $p < 0.05$

(34.8 ± 2.2, NCH), in uncontrolled diabetes (42.5 ± 1.6, DUH), or insulin-treated diabetic rats (37.7 ± 2.9, DIM).

Discussion

Immunological staining and CLSM has provided an enhanced and more precise ability to address questions of intracellular localization for particular proteins as well as localization of a given type of cells within a tissue. CLSM collects images that are almost free of out-of-focus signals, which results in improved spatial resolution compared with conventional microscopy. CLSM dramatically reduces interference from out-of-focus structures, by allowing optical sectioning of a specimen with adjustment of plane of focus. However, combination of quantitative immunological staining and confocal microscopy needs special attention regarding methodological problems. When imaging the tissue at various optical sections, particularly at the deepest layers, the measured intensity may be reduced by some excitation and emission light absorption from the more superficial tissue. These problems are much enhanced in conventional microscopy *(23)*. Relative measurements between identically treated samples eliminate the use of strict quantification in amounts of a protein, and still allow one to assess if experimental conditions resulted in a measurable relative change in the amounts of a protein. This has been our rationale for only reporting relative fluorescent intensity differences among our groups.

In normal islets, by confocal microscopy, glucagon immunoreactivity within A-cells was only found at the periphery of the islet. This is in agreement with the observation made by others using conventional microscopy *(20,21)*. Three-dimensional imaging of intact isolated islets of Langerhans with confocal microscopy showed *(24)* that A-cells were present as isolated cells or as clusters in tightly packed groups on the periphery of islets.

Only recently, quantification of a substance by fluorescent intensity measurement using digital image analysis has been possible. Labile zinc in the islet of pancreas has been visualized with specific fluorescent probe for zinc and quantified by digital image analysis *(25)*. It was found that exposure of islets to high concentration of glucose decreased labile zinc content as observed by decrease in fluorescence intensity *(25)*. In the present investigation, CLSM enabled us to quantify glucagon levels in the islet under different experimental conditions.

Morphometric analysis of islets from normal rats showed that glucagon-containing A- cell area was 20.6% of the islet area, consistent with data by conventional microscopy in rats *(20,21,26)*, dogs *(10,21)*, and humans *(20,27)*. In normal rats, there was no change in % glucagon-containing A-cell area or glucagon intensity (content)/islet during hypoglycemia from the basal state, presumably indicating increased glucagon synthesis compensating for increased glucagon release during hypoglycemia. Similar findings have been reported previously by us *(7)* and others *(14)* on glucagon content and mRNA transcripts in whole pancreas. However, in untreated diabetic rats, there was a nearly threefold increase in glucagon cell area from normal control, 19.2–20.5% (NCO, NCH) to 55–58% (DUH, DUO) with abundance of immunoreactive glucagon per islet scattered throughout the islet, indicating hyperplasia of A- cells. This is in agreement with the previous observation in rat, dog, and human *(10,20,21,26–28)*. Previous studies in diabetic rats *(21)* have shown a close relationship between increase in number of A-cells per islet and A-cell area. Therefore, in the present study, we did not count the number of A-cells, but we measured A-cell area per islet to assess A-cell hyperplasia. In the present study, we also found a two- to threefold increase in glucagon intensity per islet in DUH and DUO compared to normal rats, indicating concomitant increase in glucagon content per islet. This confirms our observation in dog *(10)*.

It is known that in physiological state, whenever there is hyperglycemia, there is a decrease in glucagon secretion owing to hyperfunction of the B-cell *(13,14,18,19,29)*. This could be owing to:

1. An increase in GABA, which is localized and secreted with insulin from B-cells in response to glucose. It acts on A-cell GABA receptor chloride channel suppressing glucagon release *(30,31)*. With impaired B-cell function, as in diabetes, there is no GABA release and, therefore, increased glucagon secretion.

2. Adrenergic stimulation is a potent stimulator of glucagon release *(32)*. Chronic hyperglycemia could be associated with decreased sympathetic activity and, therefore, decreased glucagon release.
3. Elevated circulating glucose decreases glucagon secretion by lowering intracytoplasmic CA^{++} concentration in A-cells *(33)*.
4. Finally, physiologically, increased insulin concentration both in vitro and in vivo *(13,14,18,19,29)* induced by glucose stimulation of pancreatic B-cell inhibits glucagon release via intraislet insulin effect. Accordingly, glucose can no longer inhibit glucagon release, once glucose-induced insulin secretion is lost, as in diabetes.

Collectively or separately, these factors may impair glucagon secretion during hypoglycemia, despite elevated baseline synthesis indicated by high level of glucagon content and mRNA *(7)* in diabetic islet.

We found improved glucagon response and pancreatic glucagon mRNA to acute hypoglycemia after chronic restoration of normoglycemia using phlorizin treatment in the diabetic rats *(7)*. This is substantiated by the present study. In the previous study, there was 70% of normal improvement in glucagon response in phlorizin-treated rats. This may be owing to

1. Residual defect of A-cells.
2. Normoglycemia was not maintained for sufficiently long duration.
3. An abnormality in counterregulatory hormones.

An attenuated epinephrine as well as norepinephrine response to hypoglycemia was observed in these phlorizin-treated diabetic rats *(7)* as well as in diabetic dogs *(6)*, although the mechanism of these phlorizin-related changes in catecholamines levels is unknown. A-cell responsiveness was also substantially suppressed by functional adrenalectomy in dogs *(34)*. In the present study, we found marked increase in islet glucagon content (glucagon intensity/islet area) in hypoglycemic state (DPH) compared to basal state (DPO) associated with increased glucagon concentration (glucagon intensity/A-cell area) ($p < 0.05$). These observations together with our previous studies *(7)* indicate that insulin-independent correction of hyperglycemia partially restored glucagon sensitivity in A-cell, and improved glucagon response to insulin-induced hypoglycemia by increasing glucagon synthesis, content, and secretion. In earlier studies, phlorizin-induced normoglycemia partially restored hepatic glucose production during hypoglycemia in diabetic dogs *(5,6)* and normalized the decremental glucagon response to acute hyperglycemia in untreated diabetes *(15)*. Therefore, maintenance of normoglycemia could be important in retaining A-cell glucose sensitivity to both elevated and decreased glucose levels, and for glucagon responsiveness during hypoglycemia. However, in this study, phlorizin treatment did not improve tissue insulin sensitivity in diabetic rats, since a three- to sixfold higher dose of insulin was needed to induce hypoglycemia. This may be owing to relatively short duration of the phlorizin treatment, since treatment for 4–5 wk has been reported to improve insulin sensitivity significantly in partially pancreatectomized rats *(16)*.

In contrast to phlorizin treatment, we observed a smaller and delayed increment in glucagon response to hypoglycemia after normalization of glycemia with insulin treatment. Interestingly, such insulin treatment in the present investigation resulted in 53% lower glucagon content (DPH vs DIH) during hypoglycemia. Even though the total A-cell area remained high in DIH, glucagon content per A-cell (concentration) was markedly diminished, as evidenced by lower fluorescence intensity in the confocal image. These findings support our observation in dogs *(10)*. Acute normalization of glycemia with insulin in alloxan-diabetic dogs resulted in a marked decrease in islet as well as total pancreatic glucagon content *(9,10)*. As suggested earlier, this may be owing to the inhibition of hormone gene expression *(22)*. In islets of diabetic rat, elevated levels of proglucagon mRNA were found to be reduced within 1 h of insulin administration that normalized glycemia, suggesting that insulin inhibits proglucagon gene expression either directly or via glucose *(22)*. Similar inhibitory effects of insulin on proglucagon gene transcription have been reported for a glucagon producing tumor cell line *(35)* mediated by an insulin-responsive element within the gene promoter *(36)*. Moreover, several in vivo studies also indicate that exogenous insulin inhibits islet A-cell secretion *(18,19,37,38)*. It appears that although sensitivity of A-cells to glucose is lost, sensitivity to insulin is still retained to some extent in the diabetic islet. Thus, decrease in glucagon content at the islet level observed in the present investigation may explain, in part, the impaired glucagon response to insulin-induced hypoglycemia. Therefore, besides hyperglycemia leading to impaired A-cell sensitivity, insulin treatment can also contribute to the depressed A-cell responsiveness in insulin-treated diabetics.

In our previous paper *(7)*, the extraction and measurement of glucagon from the pancreas revealed an increased glucagon content when expressed as ng/mg protein, but not as μg/g tissue in uncontrolled diabetic rats. However, this apparent increase in glucagon per mg protein was not observed in rats treated with insulin or phlorizin. This might have been owing to a decrease in protein content of pancreas in uncontrolled diabetes *(39)*, whereas in DP and DI, protein content could have been normalized owing to normalization of glycemia. The total amount of glucagon in pancreas is a product of islet glucagon content and the number of islets in the pancreas. In both dogs and rats, not only a majority of β-cells, but also up to 60% of the islets are destroyed *(8,9,21,22)*. Therefore, it is not surprising that a large increase in glucagon intensity (three to fourfold) in islets is not reflected in measurements of total glucagon content of the pancreas in diabetes. Our previous

study (7) could also not reveal changes in glucagon content during hypoglycemia presumably owing to dilution of hormonal content in large pancreatic mass. Quantification of glucagon content by confocal microscopy is much more precise than the extraction method and therefore advantageous in studies such as ours.

In conclusion, by direct measurement of intensity (glucagon content) and area of immunostained glucagon fluorescence in the islet using confocal microscopy and image analysis, we have been able to show for the first time that insulin-independent restoration of euglycemia by phlorizin increased glucagon content and concentration per islet during acute hypoglycemia. This is in contrast to untreated or insulin-treated diabetic rats, where glucagon content and concentration decreased during hypoglycemia. This finding substantiated our previous observation that insulin-independent normalization of hyperglycemia partially restored the responsiveness of A-cell with elevated basal secretion and increased synthesis and secretion of glucagon in response to hypoglycemia. Furthermore, insulin treatment reduced glucagon content of each islet especially during hypoglycemia. This may explain, at least in part, the unresponsiveness of glucagon during insulin-induced hypoglycemia in IDDM patients treated with intensive insulin therapy.

Materials and Methods

Animals

Studies were performed in the pancreas of rats reported in our previous study (7). Briefly, male Sprague Dawley rats weighing 250–300 g were used. All rats were fed rat chow (Ralston Purina Co., St. Louis, MO) and given water ad libitum. The hypoglycemic experiments were performed on 4 groups of age-matched rats:

1. Normal controls (NC, $n = 4$).
2. Untreated diabetic rats (DU, $n = 4$).
3. Diabetic rats, treated for 5 d using sustained release (2–3 U/d) insulin implant (DI, $n = 4$).
4. Diabetic rats, treated for 4 d with phlorizin (0.4 g/kg) given subcutaneously twice daily as 40% solution in propylene glycol (DP, $n = 4$).

In each group, 14–28 islets were assessed, which yielded enough data for statistical analysis. Diabetes was induced by single iv injection of 65 mg/kg body wt of streptozotocin (Sigma Chemical Co., St. Louis, MO) in 0.9% saline under pentobarbital anesthesia (50 mg/kg body wt, ip). Experiments were conducted 2 wk after induction of diabetes. In each rat, an indwelling polyethylene catheter (PE 50 Clay Adams, Boston, MA) was inserted into a carotid artery under pentobarbital anesthesia (50 mg/kg body wt, ip) for injection of insulin and for blood sampling, 3–4 d before the hypoglycemic experiment. Details of the treatments and techniques of surgery are described previously (7). All studies with animals were conducted in accordance with the guidelines of the Canadian Council for Animal Care, and the protocol was approved by the University Animal Care Committee.

Experimental Design

Acute hypoglycemia was induced in conscious, unstrained 9 to 12 h-fasted rats. At time = 0, regular insulin was injected iv with varying doses: 0.3 NC; 1.0–2.0 DU, DP, DI; U/100 g) in order to achieve comparable levels of hypoglycemia within 60 min which were then maintained for another 60 min in all groups. This was established by checking blood glucose at frequent intervals and infusing additional small dose of insulin (0.1–0.3 U/100 g) if needed. Rats were sacrificed by decapitation, and pancreas was immediately removed. Transverse section of tail portion of the pancreases was excised and fixed in 4% freshly prepared paraformaldehyde in phosphate buffer. In order to obtain baseline pancreatic tissue samples, a separate subgroup of rats ($n = 4$) from each treatment protocol (NC, DU, DP, and DI) was sacrificed at O min and designated as NCO, DUO, DPO, and DIO. Blood samples were taken before and at 15- to 30-min intervals after insulin injection via carotid canula to ascertain the hypoglycemia level. The concentration of glucose was determined from a sample of 0.01 mL plasma using a Beckman Glucose Analyzer II. Basal plasma glucose levels before iv injection of insulin were 7.4 ± 0.3 m*M* in NCO and increased to 14.5 ± 2.2 m*M* in DUO. It was normalized in DPO 5.5 ± 0.5 m*M* and DIO 6.7 ± 0.8 m*M*. The hypoglycemic levels after insulin injection at 30 min were 2.4 ± 0.1, NCH; 4.5 ± 0.4, DUH; 3.1 ± 0.2, DPH; 2.8 ± 0.2, DIH, and at 120 min 1.7 ± 0.3, NCH; 2.7 ± 0.4, DUH; 2.2 ± 0.1, DPH; and 1.6 ± 0.1 m*M*, DIH. The levels of hypoglycemia at 60 and 120 min in these groups were not significant. The corresponding plasma glucagon values were 141 ± 20, NCO; 300 ± 6.2, DUO; 450 ± 108, DPO; 189 ± 57, DIO at baseline, and at 30 and 120 min 2059 ± 311, 926 ± 61, NCH; 417 ± 132, 598 ± 88, DUH; 936 ± 183, 791 ± 180, DPH, and 552 ± 136, 651 ± 139, DIH, respectively.

Tissue Preparation and Immunofluorescence Staining

Pancreatic segments were fixed overnight at 4°C and dehydrated by passage through a graded series of alcohols, cleared in xylene and were then embedded in paraffin. Serial paraffin sections (10-μm thick) of each group before (NCO, DUO, DIO, DPO) and after hypoglycemic experiments (NCH, DUH, DIH, DPH) were simultaneously stained for glucagon using the unlabeled antibody–enzyme (peroxidase–antiperoxidase) method and counterstained with hematoxylin to facilitate nuclear identification as described before (9,10). They were kept for comparative purposes. For confocal microscopy, slides were stained by modified indirect immunofluorescence method (9,10). The sections were dewaxed and rehydrated through a series of clean xylene, graded ethanol, and water as before. The slides were then placed in 3% H_2O_2 in methanol for 20 min to

destroy tissue endogenous peroxidase activity, washed with distilled water (2 × 5 min), and phosphate-buffered saline (PBS) (2 × 5 min), and then incubated with 10% normal sheep serum (NSS) in PBS for 30 min at 24°C and finally with a 1:150 dilution of the primary antibody (rabbit antiglucagon 04A serum supplied by R. H. Unger, Dallas, TX) in PBS/1% NSS for 72 h at 4°C. The sections were then washed with PBS (3 × 5 min), incubated with a 1:30 dilution of fluorescent isothiocyanate-conjugated sheep antirabbit globulin (Jackson ImmunoResearch Inc., Westgrove, PA) for 1 h at room temperature, washed with PBS (3 × 5 min), and finally mounted with 50% glycerol in PBS containing *p*-phenylenediamine (1 mg/mL) as an antifade agent for fluorescence *(40)*. The stained sections were immediately taken for confocal microscopy.

Confocal Imaging

Confocal microscopy is a convenient approach to examine the 3-D structure of islet cells stained with particular antibodies in thick sections of tissue without having to resort to electron microscopy, which presents many problems of distortion because of the harsh fixation procedures, not to mention the problems with antibody gold labeling. In comparison to 2-D microscopy, the confocal microscopy reduces the effects of out-of-focus fluorescence contamination of the image. This error can result in large differences when quantitating fluorescent intensity of tagged antibodies. Further advantages of confocal microscopy have been described in a recent review *(41)*. In order to quantitate the glucagon immunofluorescence in the various experimental groups, the groups that produced the strongest fluorescent signals were determined to set the optimal conditions for confocal imaging of all the groups. Fluorescence imaging was obtained by use of a confocal scanning laser (Bio-Rad MRC600) mounted on an upright Nikon microscope (40× Nikon dry objective, 0.85 N.A.). The reason for this low magnification is that the majority of the islets filled the field of the scanning laser without further enhancement. Even at this magnification, it was sometimes necessary to image both halves of a large islet followed by separate quantitation of each image, and later combining the measurements for the entire islet section. For imaging, the laser beam was attenuated to 1% with a neutral density filter before passing through a blue excitation filter (488 nary). Emitted fluorescence was detected using a low-pass emission filter (515 nary). All settings were kept constant during the imaging sessions. Imaging of subsets for each group were obtained in a total of four sessions. Each session was quantitated separately, and later combined when it was determined that there were no differences in imaging intensity between sessions, by using the level of background intensity as a control. This quantitative procedure was necessary, because no independent fluorescence reference was used and there could be a measurable change in laser intensity at the same settings owing to usage over time.

In each section of tissue that was used for imaging, all of the islets present, regardless of size, were digitized. It was performed by optically sectioning the islet starting from the top and proceeding progressively to the bottom of the tissue section. The pinhole aperture size and automated *z*-axis stepping were held constant for all imaging sessions. Serial optical sections approx 1 μm each were taken through the 10-μm thick specimen. Each imaged optical section was stored as a 2-D binary image for subsequent stacking. After the stacked composite image was obtained, it was stored on optical disk for subsequent display and analysis. Since we were measuring the percentage of glucagon area per islet area, and not the size or volume of islet, we eliminated the measurement of cross-section of islet area and glucagon area in small-size islets (<1000 μm^2), which probably represented the top or bottom section of the whole islet.

The variables of interest for quantitative measures within a particular tissue section were as follows:

1. The islet cross-sectional area.
2. The cross-sectional area within the islet that stained positive for glucagon.
3. The total fluorescence intensity of the islet cross-sectional area.
4. The fluorescence intensity of the cross-sectional area within the islet that stained positive for glucagon.

The intensity of the same amount of area outside the islet was used as background subtraction. All glucagon fluorescent intensity measures were subtracted from intensity of the same amount of background area. Fluorescence intensity was expressed as gray scale units. Cross-sectional areas of islet and glucagon positive cells in μm^2 were measured by outlining the area on the monitor displaying the image with the use of a cursor and Bio-Rad software or software by Babak Jahromi, University of Toronto, and percentage of glucagon area/islet area was calculated. Since glucagon-containing-A cells are mostly on the periphery of the islet, the marginal cross-sections of the islet will undoubtedly over estimate glucagon area and its proportion in the entire islet area. Moreover, in a smaller size islet, measurement of the glucagon area may not be accurate. The software analysis also provided the total and averaged fluorescence intensity (total intensity/islet area and total intensity/glucagon area) of outlined areas, indicating glucagon content per islet area and glucagon content per A-cell area (concentration). Images were rendered in pseudocolor for visual assessment. The most common method of assigning color to intensity images is by thresholding. Various intensity ranges are assigned different colors, with the color in each range usually being ranked from dark to light to reflect fluorescence intensity. Red denoted maximum intensity, followed by yellow, green, light blue and dark blue. All the quantitative analysis and image processing were performed from a SUN workstation provided by Tom Goldthorpe.

Data for each experimental group were combined to obtain values of both mean and standard error of the mean. Statistical analysis was performed between individual groups by the Kruskal-Wallis one-way analysis of variance on ranks and to isolate the groups that differ from others, pairwise multiple comparison procedures (Dunn's method) were used at $p < 0.05$ level. The measured distributions were plotted in a rank order frequency histogram. Since 3-D serial reconstructions of individual islets were not performed in this study, the distributions from random 2-D sections were used to determine trends in size differences among islet between groups. This approach in plotting distributions is necessary when considering stereological problems of measurements obtained from random 2-D profiles of 3-D objects *(42,43)*.

Acknowledgments

The authors are grateful to D. Bilinski, M. VanDelangeryt, and L. Lam for excellent technical assistance and L. Vranic for secretarial help. We thank the MRC group, Nerve Ceils and Synapses, at the University of Toronto for use of the confocal microscope. We thank Paul Wang, University of Toronto, for supplying the Linplant insulin implants. This work was supported by the Medical Research Council of Canada, and Canadian Diabetes Association to M. V. It was presented in part at the 75th anniversary: Celebrating the Discovery of Insulin, Toronto, Canada 1996. Q. S. was supported by Banting and Best Diabetes Centre Scholarship, University of Toronto. Current address: Amgen Inc., Thousand Oaks, CA. RLC Postdoctoral Fellowship from Network Centres of Excellence (Canada). Current address: School of Biological Science, Div. of Organisms & Integrative Biology, University of Kentucky, Lexington, Kentucky, 40506-0225.

References

1. Kleinbaum, J. and Shamoon, H. (1983). *Diabetes* **32,** 493–498.
2. Cryer, P. E., Binder, C., Bolli, G., Cherrington, A. D., Gale, E. A. M., Gerich, J. E., et al. (1989). *Diabetes* **38,** 1193–1199.
3. Orskov, L., Alberti, K. G. M. M., Mengel, A., Moller, N., Pedersen, O., Rasmussen, O., et al. (1991). *Diabetologia* **34,** 521–526.
4. Bolli, G., Calabrese, G., and De Foe, P. (1982) *Diabetologia* **22,** 100–105.
5. Lussier, B., Vranic, M., Kovacevic, N., and Hetenyi, G. Jr. (1986). *Metabolism* **35,** 18–24.
6. Hetenyi, G., Jr, Gauthier, C., Byers, M., and Vranic M. (1989). *Am. J. Physiol.* **256,** E277–E283.
7. Shi, Z. Q., Rastogi, K. S., Lekas, M., Efendic, S., Drucker, D. J., and Vranic, M. (1996). *Endocrinology* **137,** 3193–3199.
8. Patel, D. G. (1983). *Metabolism* **32,** 377–382.
9. Rastogi, K. S., Lickley, L., Jokay, M., Efendic, S., Vranic, M. (1990). *Endocrinology* **126,** 1096–1104.
10. Rastogi, K. S., Brubaker, P. L., Kawasaki, A., Efendic, S., and Vranic, M. (1993). *Can. J. Physiol. Pharmacol.* **71,** 512–517.
11. Cerasi, E., Luft, R., and Efendic, S. (1972). *Diabetes* **21,** 224–234.
12. Gerich, J. E., Langiois, M., Noacco, C., Karam, J. H., and Forsham, P. H. (1973). *Science* **182,** 171–173.
13. Dimitriadis, G., Cryer, P., and Gerich, J. (1985). *Diabetologia* **28,** 63–69.
14. Magnam, C., Philippe, J., Kassis, N., Laury, M. C., Penicaud, L., Gilbert, M., and Ktorza, A. (1995). *Endocrinology* **136,** 5370–5376.
15. Starke, A., Grundy, S., McGarry, J. D., and Unger, R. H. (1985). *Proc. Natl. Acad. Sci. USA* **82,** 1544–1546.
16. Rossetti, L., Smith, D., Shuman, G. I., Papachristou, D., and DeFronzo, R. A. (1987). *J. Clin. Invest.* **79,** 1510–1515.
17. Ensinck, J. W. and Kanter, R. A. (1980). *Diabetes Care* **3,** 285–289.
18. Unger, R. H. (1983). *Diabetes* **32,** 575–583.
19. Muller, W. A., Faloona, G. R., and Unger, R. H. (1971). *J. Clin. Invest.* **50,** 1991–1999.
20. Patel, Y. C., Cameron, D. P., Bankier, A., Malaisse-Lagae, F., Ravazzola, M., Studer, P., et al. (1978). *Endocrinology* **103,** 917–923.
21. Orci, L., Baetens, D., Rufener, C., Amherdt, M., Ravazzola, M., Studer, P., et al. (1976). *Proc. Natl. Acad. Sci. USA* **73,** 1338–1342.
22. Chen, E., Komiya, I., Inman, L., McCorkle, K., Alan, T., and Unger, R. H. (1989). *Proc. Natl. Acad. Sci. USA* **86,** 1367–1371.
23. Peterson, N. O., Hoddelius, P. L., Wiseman, P. W., Seger, O., and Magnusson, K. E. (1993). *Biophys. J.* **65,** 1135–1146,
24. Brelje, T. C., Scharp, D. W., and Sorenson, R. L. (1989). *Diabetes* **38,** 808–814.
25. Zalewski, P. D., Millard, S. H., Forbes, I. J., Kapaniris, O., Slavotinek, A., Bett W. H., et al. (1994). *J. Histochem. Cytochem.* **42,** 877–884.
26. Parsons, J. A., Hartfel, M. A., Hegre, D. D., and McEvoy, R. C. (1983). *Diabetes* **32,** 67–74.
27. Koozulinko, S., Soejima, K., and Landing, BH. (1986). *Ped. Pathol.* **6,** 25–46.
28. Stefan, Y., Orci, L., Malaisse-Lagae, F., Perralet, A., Patel, Y. C., and Unger, R. H. (1982). *Diabetes* **31,** 694–700
29. Greenbaum, C. J., Havel, P. J., Taborsky, G. J., and Klaff, L. J. (1991). *J. Clin. Invest.* **88,** 767–773.
30. Garry, D. J., Sorenson, R. L., and Coulter, H. D. (1987). *Diabetologia* **30,** 115–119.
31. Rorsman, P., Berggren, P. O., Bokorst, K., Ericson, H., Mohler, H., Ostenson, C. G., and Smith, P. A. (1989). *Nature* **341,** 233–236.
32. Havel, P. J., Veith, R. C., Dunning, B. E., and Taborsky, G. J. Jr. (1991). *Diabetes* **40(9),** 1107–1114.
33. Johansson, H., Gylfe, E., and Hellman, B. (1987). *Biochem. Biophys. Res. Comm.* **147,** 309–314.
34. Yamaguchi, N., Briand, R., and Gaspo, R. (1990). *Can. J. Physiol. Pharmacol.* **68(9),** 1183–1188.
35. Phillippe, J. (1981). *J. Clin. Invest.* **84,** 672–677.
36. Phillippe, J. (1991) *Proc. Natl. Acad. Sci. USA* **88,** 7224–7227.
37. Ito, K., Maruyama, H., Hirose, H., Kido, K., Koyama, K., Kataoka, K., et al. (1995). *Metabolism* **44(3),** 358–362.
38. Liu, D., Adamson, U. C. K., Lins, P. E. S., Kollind, M. E., Moberg, E. A. R., and Andreasson, K. (1992). *Diabetes Care* **15,** 59–65.
39. Kimball, S. R., Vary, T. C., and Jefferson, L. J. (1994). *Ann. Rev. Physiol.* **56,** 321.
40. Johnson, G. D., Davidson, R. S., McNamee, K. C., Russell, G., Goodwin, D., and Holborow, E. J. (1982). *J. Immunol. Methods* **55,** 231–242.
41. Shotton, D. M. (1989). *J. Cell Sci.* **94,** 175–206.
42. Guz-Olive, L. M. and Weibel, E. R. (1990). *Am. J. Physiol.* **258,** L148–L156.
43. Atwood, H. L. and Cooper, R. L. (1996) *J. Neurosci. Methods* **69,** 51–58.